



Contents lists available at ScienceDirect

Journal of Neuroscience Methods

journal homepage: www.elsevier.com/locate/jneumeth



Basic Neuroscience

Effects of time lag and frequency matching on phase-based connectivity

Michael X Cohen

Department of Psychology, University of Amsterdam, Netherlands

ARTICLE INFO

Article history:

Received 30 June 2014

Received in revised form 6 September 2014

Accepted 6 September 2014

Available online xxx

Keywords:

EEG connectivity
Phase clustering
Phase-locking value
Phase lag index
Laplacian
Oscillations

ABSTRACT

The time- and frequency-varying dynamics of how brain regions interact is one of the fundamental mysteries of neuroscience. In electrophysiological data, functional connectivity is often measured through the consistency of oscillatory phase angles between two electrodes placed in or over different brain regions. However, due to volume conduction, the results of such analyses can be difficult to interpret, because mathematical estimates of connectivity can be driven both by true inter-regional connectivity, and by volume conduction from the same neural source. Generally, there are two approaches to attenuate artifacts due to volume conduction: spatial filtering in combination with standard connectivity methods, or connectivity methods such as the weighted phase lag index that are blind to instantaneous connectivity that may reflect volume conduction artifacts. The purpose of this paper is to compare these two approaches directly in the presence of different connectivity time lags (5 or 25 ms) and physiologically realistic frequency non-stationarities. The results show that standard connectivity methods in combination with Laplacian spatial filtering correctly identified simulated connectivity regardless of time lag or changes in frequency, although residual volume conduction artifacts were seen in the vicinity of the “seed” electrode. Weighted phase lag index under-estimated connectivity strength at small time lags and failed to identify connectivity in the presence of frequency mismatches or non-stationarities, but did not misidentify volume conduction as “connectivity.” Both approaches have strengths and limitations, and this paper concludes with practical advice for when to use which approach in context of hypothesis testing and exploratory data analyses.

© 2014 Elsevier B.V. All rights reserved.

1. Introduction

Brain functional connectivity is a topic of growing interest in neuroscience (Sporns, 2010; Hutchison et al., 2013; Cabral et al., 2014). In humans, functional connectivity can be measured using either hemodynamic (fMRI) or electrophysiological (MEG or EEG) techniques. Noninvasive electrophysiological measurements of functional connectivity have two main advantages: They measure changes in connectivity in a time-frame that matches that of many cognitive/perceptual processes (tens to hundreds of ms), and they can be more easily linked to underlying neurophysiology compared to the hemodynamic response.

The main disadvantage of measuring electrophysiological functional connectivity is that there is a potential confound of volume conduction. Volume conduction is the phenomenon that electromagnetic fields generated at a location in the brain will propagate through tissues (brain, skull, skin, etc.) and will be recorded from

several electrodes. Volume conduction is a double-edged sword: Without it, non-invasive M/EEG would not be possible; because of it, functional connectivity measurements can be confounded.

The question is thus how to dissociate volume conduction from true interactions between brain regions when estimating functional connectivity. Broadly speaking, there are two approaches for this dissociation. The first approach is to develop data analysis methods that are blind to the potential influence of volume conduction. This has led to methods such as (corrected) imaginary coherence (Nolte et al., 2004; Sekihara et al., 2011) and (weighted) phase-lag-index (Stam et al., 2007; Vinck et al., 2011). The second approach is to apply spatial filters to the data that strongly attenuate volume conduction and therefore permit the valid interpretation of standard connectivity analysis methods. The most commonly used scalp-level spatial filter for this approach is the surface Laplacian (Srinivasan et al., 2006).

It appears that these two approaches reflect different “camps” of thinking about how to perform connectivity analyses. The purpose of this paper is to examine the advantages and disadvantages of these two approaches for EEG connectivity analyses. Part of the

E-mail address: mikexcohen@gmail.com

motivation for this study is based on informal scientific interactions (i.e., those that do not take place in peer-reviewed publications); I frequently hear or read researchers offering advice or demanding re-analyses of connectivity findings based on their idea of how best to address the volume conduction issue. In many cases, these suggestions seem to be based on a poor understanding of the advantages and limitations of different approaches and connectivity analysis methods. This misunderstanding can lead to misguided interpretations of findings, good-intentioned but poor advice, or inappropriate reviewer demands.

There are many methods to quantify functional connectivity in M/EEG time series. The focus of this paper is on phase-based connectivity methods, because they are widely used in the literature, and because phase-based connectivity is more often highlighted in theoretical and computational discussions of how disparate neural circuits might interact (Bush and Sejnowski, 1996; Varela et al., 2001; Fries, 2005). Two phase-based connectivity methods will be compared here: phase clustering and weighted phase lag index. Phase clustering is based on the circular variance of phase angle differences; phase lag index, in contrast, is based on the average number of phase angle differences that are positive or negative in the complex plane (that is, pointing up or down with respect to the horizontal real axis).

Phase clustering and phase lag index are sometimes mistakenly considered to be roughly equivalent with the latter being insensitive to volume conduction. This is true only in the narrow situation of tight clustering with a time lag close to $\pi/2$ (or $-\pi/2$), and very little noise. In real data, there are at least two phenomena that produce notable differences between phase clustering and phase lag index. The first is small time lags, which, in combination with noise, can cause a distribution of phase angles to be close to 0 or π . Phase clustering is insensitive to time lags, but phase lag index will produce lower estimates of connectivity as the distribution gets closer to 0 or π . This can be particularly problematic if the time lag or the amount of noise differs over time or across conditions. The second phenomenon is violations of frequency stationarity. Frequency stationarity means that the frequency characteristics of a signal remain constant over time. Although EEG is often conceptualized (or, at least, analyzed) as comprising temporally overlapping stationary oscillators, in fact the frequency structure of EEG changes dynamically over time: different brain regions oscillate at different sub-frequencies (e.g., peak alpha can be 8 Hz in one region and 9 Hz in another region) (Tognoli and Kelso, 2013), peak oscillation frequency varies as a function of task demands (Roberts et al., 2013; Haegens et al., 2014), and peak frequency can fluctuate over time due to endogenous and experimental factors (Ahissar et al., 2001; Foffani et al., 2005; Ray and Maunsell, 2010; Cohen, 2014a). Although part of the frequency non-stationarities might simply reflect measurement noise, non-stationarities are a meaningful feature of brain function that should be considered and incorporated into analyses, rather than ignored (Kaplan et al., 2005).

The idea of this study was to simulate EEG data that include a time period of frequency band-specific synchronization of several hundred ms. Data were simulated in two brain dipoles and then projected onto 64 points on the scalp, thus simulating a typical 64-channel EEG recording setup. Thereafter, data were re-referenced to the average of all electrodes, or were spatially filtered using the Laplacian. Real EEG data were also used from a previously published study. Functional connectivity was then estimated via phase clustering and weighted phase lag index. The two independent variables were the time lag between the simulated interactions (5 or 25 ms) and the frequency stationarity and matching of the two dipoles.

I argue in this paper that the choice of phase-based functional connectivity analyses for EEG data should be based in part on the relative aversion to Type-I vs. Type-II errors, which in turn should be

guided by whether the analyses are relatively hypothesis-driven vs. exploratory. To quell suspense, the results of analyses of simulated and real EEG data show: (1) weighted phase lag index should be preferred in exploratory studies whereas phase clustering should be preferred in hypothesis-driven studies; (2) if one is interested in the time course of changes in connectivity, phase clustering should be preferred, because even minor violations of frequency stationarity cause connectivity estimation errors for weighted phase lag; (3) the surface Laplacian renders connectivity estimates robust to time lag and frequency non-stationarities, although the Laplacian remains open to volume conduction confounds for closely positioned electrodes (<5 cm when using a standard 64-channel cap).

Matlab code to produce these simulations and analyze the results are posted online (www.mikexcohen.com/Cohen.phaseConnectivityComparison.zip). Readers are encouraged to inspect the results for themselves, modify parameters, etc.

2. Methods

2.1. Methods for estimating phase-based connectivity

Inter-site phase clustering (ISPC; also known as phase-locking value/factor, phase coherence, and several other terms; ISPC is preferred here because it is a description of the analysis rather than an interpretation of the result; see Cohen, 2014b) is defined as the length of the average of phase angle difference vectors from two electrodes: $n^{-1} \sum e^{ip}$, where n is the number of data points (here, trials), e is the natural exponential, i is the imaginary operator (the square root of -1), and p is the phase angle difference in radians between two electrodes.

The weighted phase lag index (wPLI; Vinck et al., 2011) is based on the phase lag index (PLI; Stam et al., 2007), which defines connectivity as the absolute value of the average sign of phase angle differences (+1 or -1 , relative to the real axis; thus, a population of 3 positive vectors and 1 negative vector would have a PLI value of 0.75). The wPLI modifies the PLI by deweighting vectors that are closer to the real axis such that those vectors have a smaller influence on the final connectivity estimate.

Although wPLI and ISPC are occasionally informally discussed as equivalent phase-based measures of connectivity with the exception that wPLI is insensitive to volume conduction, this is actually not the case. ISPC is based purely on the amount of clustering of phase angle differences (this can be thought of as variance of vectors in a circle) regardless of their absolute orientation with respect to the real axis. In contrast, wPLI is based on the weighted number of phase angle differences that are either positive or negative (that is, whether the vectors point “up” or “down” on a polar plot with the real axis as a horizontal line), and is only somewhat affected by the amount of clustering, depending on the relation of the cluster with respect to the real axis. ISPC and wPLI can thus be doubly dissociated, as illustrated in Fig. 1.

2.2. Simulation of EEG data

Simulated data can range in biophysical plausibility, from detailed conductance-based models that produce biophysically interpretable M/EEG signals to simple sinusoidal models. The amount of biophysical plausibility required depends on the purpose of the simulation. Because the purpose of this study is to investigate the implications of spatial filtering and analysis methods on estimated connectivity, rather than to understand the mechanisms or implications of phase connectivity for neural computations, a relatively simple simulation utilizing fewer biophysical parameters is preferable.

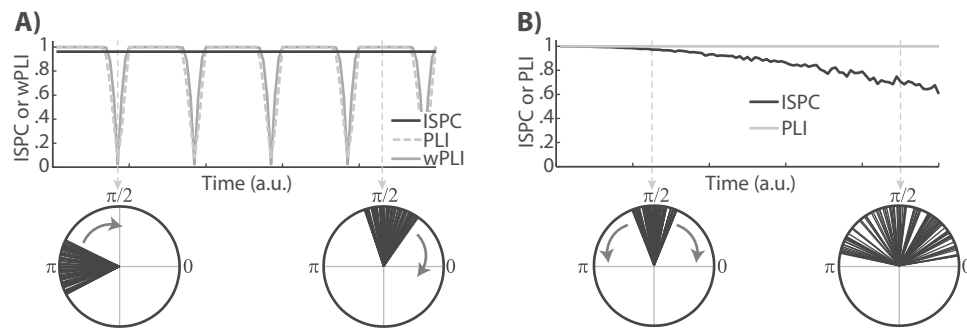


Fig. 1. Dissociation between two methods of measuring phase-based functional connectivity. ISPC (inter-site phase clustering) reflects the variance of phase angle differences whereas PLI (phase-lag index) reflects the proportion of phase angle differences above or below the real (horizontal) axis. In panel A, simulated connectivity had the same clustering but cycled around the polar plane (see lower polar plots); this phenomenon occurs when there is a subtle frequency mismatch between the two oscillators, and occurs in real neural data. The top plot shows time courses of connectivity. ISPC (thin black line) remained constant over time, while the PLI and wPLI exhibited large fluctuations corresponding to the distribution crossing the real axis (0 or π). Panel B shows a different scenario, in which the phase angle differences remained above the real axis but the variance increased over time (see lower polar plots). The PLI remains at 1.0 throughout because it is sensitive only to the proportion of phase angles that point to one side of the real axis. In contrast, ISPC decreases because it reflects the variance of the phase angle distribution, which increased over time.

Thus, 2004 time series, comprising random numbers and corresponding to spatially distributed gray matter dipoles, were generated. Two dipoles, one in medial prefrontal cortex and one in medial occipital cortex (Fig. 2), were selected to be the “activation dipoles,” and their time courses were simulated as Gaussian-tapered sine waves plus noise. In theory, each brain voxel can be represented as a 3D vector corresponding to the three cardinal orientations (X, Y, and Z, with respect to the standard MNI coordinates); data were here simulated only on the Z axis for simplicity (that is, both dipoles were pointing “up”). The online Matlab code provides instructions for testing the simulations using dipoles pointing in different directions; this is useful to understand how opposite sides of a single dipole can produce spurious anti-phase connectivity. The sampling rate was 200 Hz, and 300 trials were used. Preliminary inspection suggested that the results presented here were fairly stable after ~50 trials; more trials are useful to increase the signal-to-noise ratio.

To simulate connectivity, the occipital dipole time series on each trial was computed by adding a sine wave to the prefrontal dipole, with a random phase jitter of between 0 and $\pi/10$, plus either 5 ms or 25 ms in different runs to simulate short- or long-time lag connectivity.

Eight sets of simulations were run by changing the frequency and time-lag characteristics (Fig. 3). In simulation 1, both dipoles oscillated at a constant 10 Hz. In simulation 2, the prefrontal dipole oscillated at a constant 10 Hz while the occipital dipole oscillated at a constant 12 Hz. In simulation 3, the average frequency of both dipoles over time was 10 Hz, but the frequency varied randomly over time. The range of the frequency variation was 9–11 Hz (simulation 3a) or 8–12 Hz (simulation 3b). Note that in simulation 3, the trial-average frequencies appear highly stationary over time and are close to a flat line at 10 Hz. However, within each trial the frequencies varied over time. Each of these four simulations was run using a 5 ms or 25 ms time lag between the prefrontal and the occipital dipoles.

After generating source-level dipole activity, the time series at each voxel were projected to 64 scalp electrodes (Fig. 2) using a forward model that was created based on the MNI template MRI in the Matlab toolbox Brainstorm (Tadel et al., 2011) with the openmeeg algorithm (Gramfort et al., 2010). Scalp EEG data were stored separately for average reference and for the surface Laplacian.

2.3. Real EEG data

EEG data were taken from a recent study (Cohen, 2014c). Briefly, 29 human volunteer subjects performed a speeded reaction time

task in which they responded according to the central letter of a 5-letter string while ignoring the flanking letters. The flankers were either congruent (e.g., “TTTTT”), 50% incongruent (e.g., “IITTT”) or fully incongruent (e.g., “IITII”). The task was modeled after the task used in Appelbaum et al. (2011), including trial timing and stimulus sizes. EEG data were recorded from 64 electrodes using Biosemi hardware (www.biosemi.com). Data were cleaned by visual trial inspection/rejection and by independent components analysis in eeglab (Delorme and Makeig, 2004). Only commission errors (trials in which the subject pressed the incorrect button) were used for the analyses here. Subjects performed ~1500 trials in total, and there were on average 174 error trials per subject (range: 47–393).

2.4. Data analyses

Time series data were converted to the time–frequency domain via convolution with a family of complex Morlet wavelets, defined as Gaussian-tapered complex sine waves. Twenty-five logarithmically spaced frequencies between 2 and 40 Hz were used. The number of cycles increased from 3 to 12 in logarithmic steps. Convolution was performed via frequency-domain multiplication, in which the Fourier-derived spectrum of the EEG data was multiplied by the spectrum of the wavelet, and the inverse Fourier transform was taken. Power and phase were defined as, respectively, the squared magnitude of the complex result and the angle relative to the positive real axis.

3. Results

3.1. Selected dipoles, scalp projections, and reconstructions

Fig. 2b–d shows the topographical distributions of the individual leadfield projections from each of two selected “activation dipoles,” the summed leadfield projections, and their Laplacian. Time series were then generated at the two dipoles as tapered alpha (10 Hz) oscillations. Time–frequency and beamforming analyses revealed that the topographical and spatial distributions of the results mapped well onto the individual dipole locations (Fig. 2a). These are not surprising results, but demonstrate that (1) the topographical and beamforming analyses (and, thus, the leadfield) produce reasonable and accurate results, and (2) the Laplacian successfully isolates the overlapping activity from the two dipoles. When the simulated dipoles were highly temporally coherent and with small time lag, the beamforming results had decreased power due to signal source suppression (Seki-hara et al., 2002), while the Laplacian was relatively unaffected (data not shown).

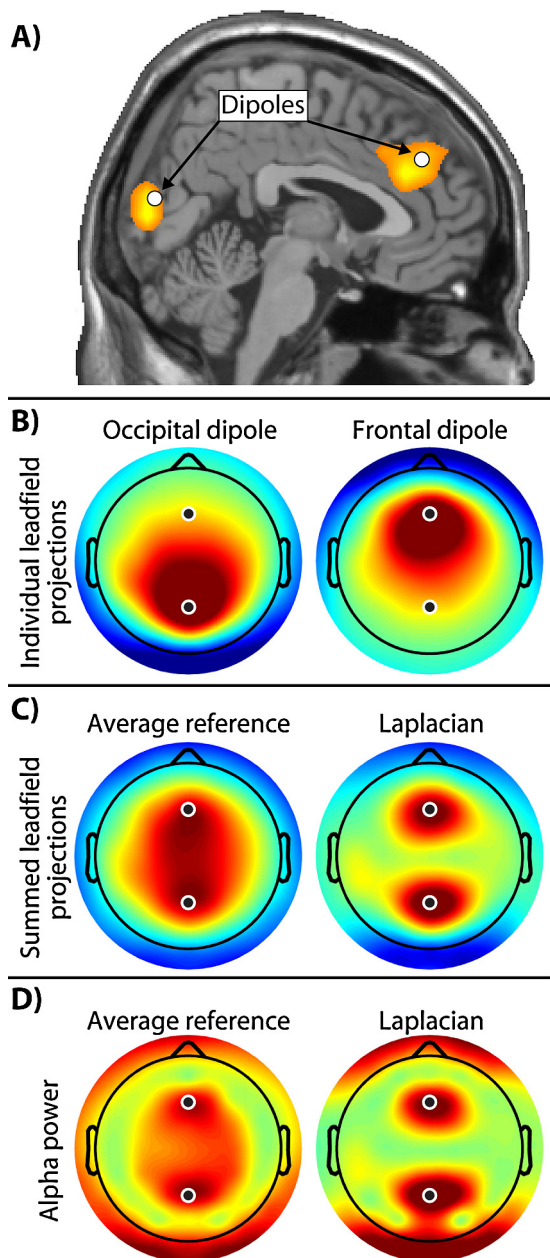
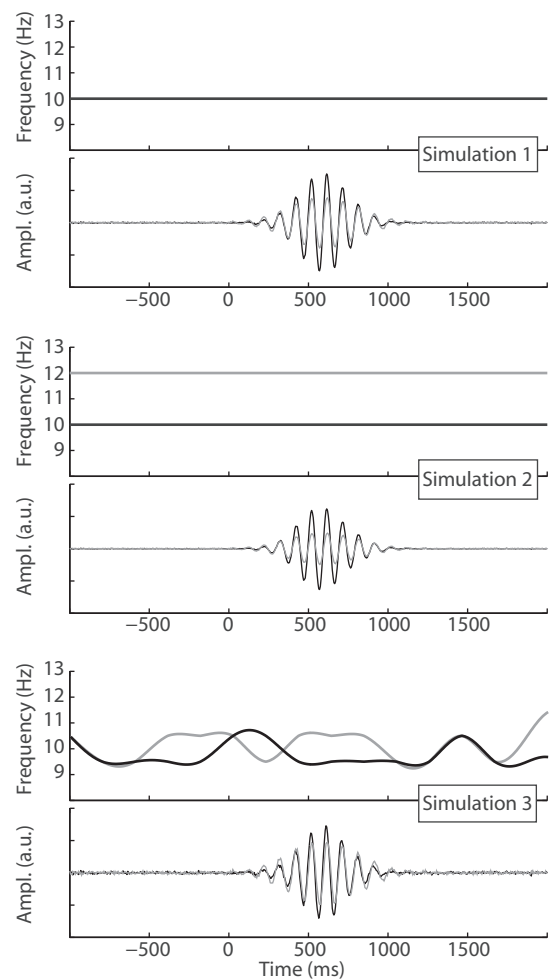


Fig. 2. Locations and projections of “activation dipoles.” Panel A shows the approximate locations of the two dipoles (white circles) on the MRI, as well as the alpha-band power resulting from a beamforming analysis (orange/yellow color, thresholded at 2 dB). The voxels were 10 mm³ and were upsampled to the MRI resolution for display (1 mm³). Panel B shows the scalp projections of the two dipoles. Panel C shows the summed projections of both dipoles using an average reference or surface Laplacian. The Laplacian is a spatial band-pass filter, which, for 64 electrodes, effectively is a high-pass filter. Panel D shows results of a time–frequency analysis (alpha band shown) on the simulated time series. Note that the red activity around the edges of the topographies are not artifacts, but instead reflect the opposite side of the dipole projections (see blue regions in panels B–C). (For interpretation of the references to color in this figure legend, the reader is referred to the web version of the article.)

Based on these results, subsequent scalp-level connectivity analyses were computed between electrodes Fz and Pz (see black/white dots on topographical maps). The dipole projection maps in Fig. 2c–d suggest that one can imagine a horizontal line connecting the two ears (thus following the “C” electrodes); any Fz-seeded connectivity anterior to this line can be considered an artifact of volume conduction.

A) Spectrotemporal characteristics of simulated data



B) Example real EEG data (N=1, electrode Oz)

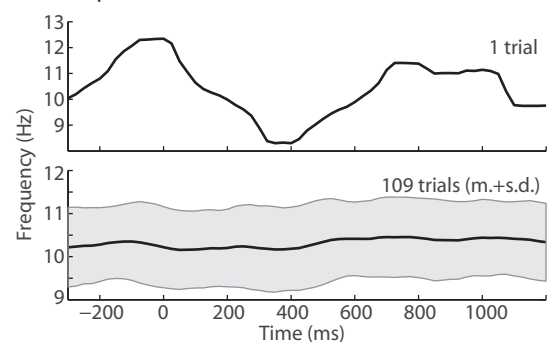


Fig. 3. Panel A illustrates how the time series were generated for the three simulations. Time series were generated by Gaussian-tapered sine waves. Connectivity was created by having the time series of the second (gray lines) dipole be a function of that of the first (black lines) dipole. In each pair of plots, the upper plot shows the frequency of the oscillators over time while the lower plot shows an example trial time course. In simulation 1, the frequency of both oscillators was a constant 10 Hz (black and gray lines are overlapping in the upper plot). In simulation 2, the frequency of both oscillators was constant over time at 10 Hz and 12 Hz. In simulation 3, the frequencies of both oscillators fluctuated randomly over time and on each trial with a mean of 10 Hz and a dispersion of either 2 (9–11 Hz; simulation 3a, depicted here) or 4 (8–12 Hz; simulation 3b). Panel B illustrates that time-varying changes in peak oscillation frequency (frequency sliding) occur in real EEG data, in the dispersion range of simulation 3b. The upper panel shows peak alpha frequency over time for one trial, and the lower panel shows mean peak frequency and one standard deviation ($m + s.d.$) over 109 trials in one human subject.

3.2. Connectivity in simulation 1 (Fig. 4)

In simulation 1, both dipoles oscillated at a constant 10 Hz. Both ISPC and wPLI successfully identified the simulated connectivity, although with 5 ms time lag, wPLI underestimated the connectivity by approximately 40% – that is, the connectivity estimate for 5 ms lag was ~60% of the connectivity estimate for 25 ms lag although the amount of clustering was the same.

Topographical maps of Fz-seeded connectivity showed that the wPLI successfully topographically isolated the posterior dipole without incorrectly identifying frontal electrodes as showing connectivity. The wPLI on the Laplacian-transformed data produced a similar but more topographically isolated effect. Seeded ISPC topographical maps correctly identified the posterior dipole but additionally showed artifactual connectivity surrounding the seed electrode, reflecting volume conduction (connectivity anterior to the “ear-to-ear line” as described in the previous subsection).

3.3. Connectivity in simulation 2 (Fig. 5)

In simulation 2, both dipoles had a constant frequency, but one was faster than the other (10 Hz and 12 Hz). Both ISPC and wPLI successfully identified the connectivity. However, wPLI produced large transient fluctuations in time courses that were driven by the phase angle distributions crossing 0 and π (see Fig. 1a). There were also small dips in the ISPC time series.

The topographical maps appeared fairly similar to those in Fig. 4, although the wPLI was weaker due to the large transient dips.

3.4. Connectivity in simulations 3a–b (Figs. 6 and 7)

In simulation 3, both dipoles oscillated with changing frequencies over time, with a mean of 10 Hz. In simulation 3a, the range of frequency non-stationarities was 9–11 Hz, and in simulation 3b, the range was 8–12 Hz. ISPC successfully identified the connectivity in both simulations, although the strength of the connectivity was around 75% compared to the simulations with stationary oscillators. This was roughly equivalent regardless of the time lag or range of frequency non-stationarities (simulations 3a vs. 3b).

wPLI largely failed to identify the connectivity, with the time series of connectivity showing small increases that are approximately the same magnitude as the pre-trial increases, which are attributable to random noise. The larger the frequency non-stationarity, the worse the wPLI estimate. With smaller frequency variance than shown here (1 Hz or less), the wPLI was able to identify the connectivity albeit with weak estimates (Fig. 8).

3.5. Connectivity in real EEG data

In the final set of analyses, ISPC and wPLI were evaluated using real EEG data. Data were taken from an existing dataset (Cohen, 2014c); connectivity was computed between FCz and Pz during trials in which human subjects made response errors during a speeded reaction time task. Electrode FCz was selected because it generally is the spatial peak of conflict- and error-related theta-band activity during speeded reaction-time tasks, including in the original dataset (Cohen, 2014c). Connectivity with Pz was evaluated because the connectivity was stronger for errors compared to correct responses, and had a non-zero time lag. The time course of connectivity at 6 Hz is shown for each of 29 subjects individually, and averaged across the group, in Fig. 9. Note the temporally variable estimates of connectivity with wPLI that, for some subjects, “bounced” toward and away from zero. Because the time course of these fluctuations was variable across subjects, group-averaged wPLI result was smoother, though lower in magnitude compared to

ISPC. Averaging the wPLI across several frequency bands smoothed the phasic dips to some extent (data not shown).

4. Discussion

4.1. Phase clustering vs. weighted phase lag index for EEG connectivity

These results paint a nuanced picture of ISPC vs. wPLI for measuring functional connectivity. ISPC is robust both to time lags and to frequency non-stationarities, but can also be misled by volume conduction artifacts. wPLI, on the other hand, is insensitive to volume conduction artifacts, but can underestimate the strength of connectivity with realistically small time lags and can produce uninterpretable connectivity time courses in the presence of frequency mismatches or non-stationarities (which occur in real EEG data, discussed more below). ISPC and wPLI will produce the same results only in the narrow situation of nearly perfectly matched frequencies and large inter-regional time lags. It is more realistic, however, that ISPC and wPLI will provide at least somewhat divergent results due to volume conduction, small time lags, noise, and frequency non-stationarities.

Specific recommendations for when to use which method are discussed later. Importantly, the theoretical demonstrations, simulations, and empirical data analyses provided here clearly show that while ISPC and wPLI are both powerful and useful measurement tools, they should not be considered equivalent, nor is either appropriate as a one-size-fits-all connectivity measure.

4.2. Effects of spatial filtering on phase-based connectivity

The topographical maps clearly show that the Laplacian is superior to the average reference for attenuating artifacts attributable to volume conduction. This is consistent with several previous simulation and empirical studies (Srinivasan et al., 2007; Winter et al., 2007; Cohen, 2014c). Thus, the Laplacian transform is strongly recommended for interpreting ISPC connectivity analyses. However, it is equally clear that the Laplacian does not completely eliminate volume conduction artifacts. All Laplacian ISPC topographical maps showed strong “connectivity” in the electrodes directly surrounding the seed electrode. Thus, ISPC in combination with the Laplacian will still produce false positives in the vicinity of the seed electrode. It is recommended to avoid interpreting connectivity in electrodes that are physically close to the seed electrode. The definition of “close” depends several factors including the smoothing parameter of the Laplacian, the number and density of electrodes, and the location and strength of the dipole with respect to the electrodes. For a 64-channel cap, interpreting connectivity within ~5 cm of the seed electrode should be avoided.

Although the Laplacian is not necessary for interpreting results from the wPLI, it nonetheless may be useful to facilitate topographical localization. For example, the average reference topographical maps for wPLI suggested broad centro-parietal connectivity with Fz, but the Laplacian more accurately localized this connectivity to parietal electrodes.

4.3. Effects of frequency non-stationarities on phase-based connectivity

The problem of frequency non-stationarities for the wPLI was illustrated in Fig. 1a: if one oscillator has a slightly different frequency than the other, the distribution of phase angle differences will “spin” around the polar plane; as the distribution crosses 0 or π , wPLI (as well as other phase-lag-based measures such as PLI, dwPLI, imaginary coherence, and corrected imaginary coherence)

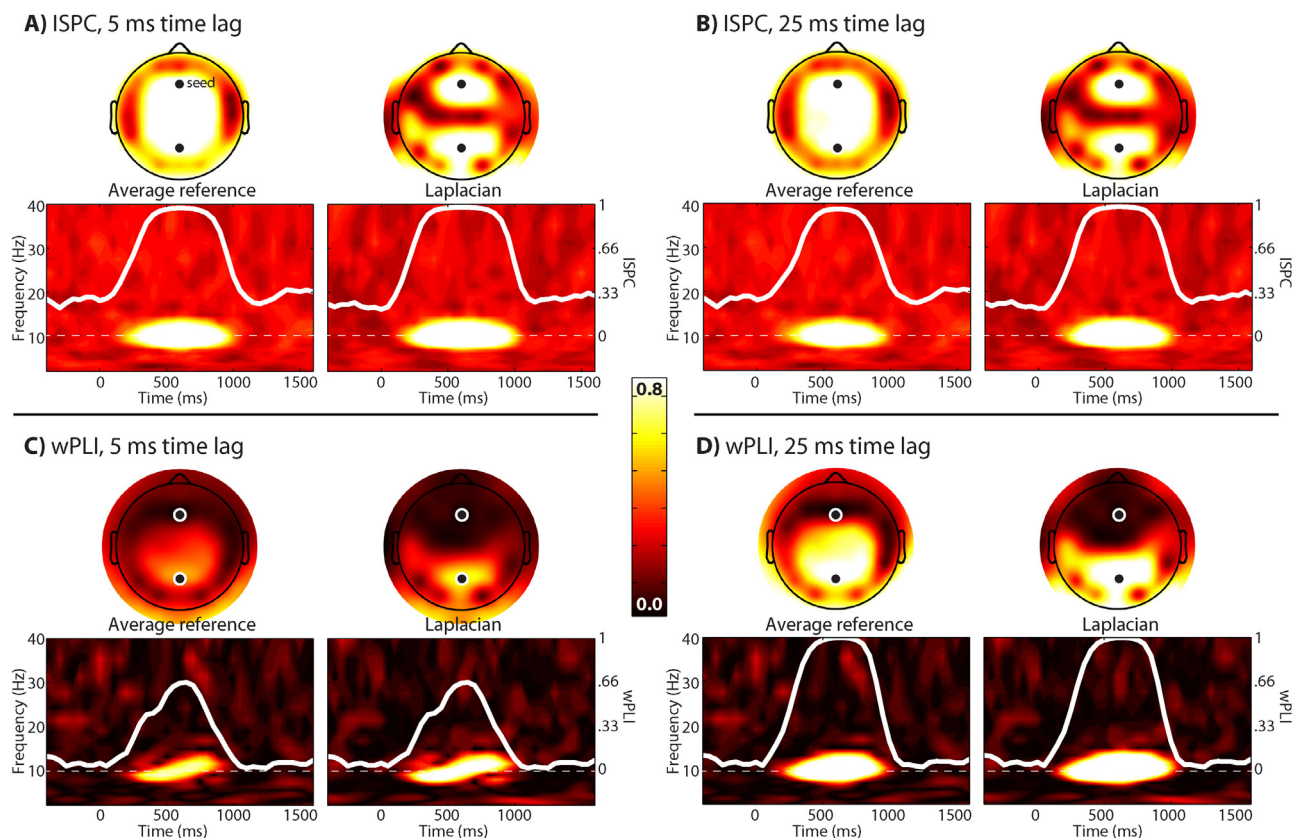


Fig. 4. Results of simulation 1 (both oscillators at a constant 10 Hz). Panels A and B show connectivity estimates from ISPC, and panels C and D show connectivity estimates from wPLI; panels A and C show results when the connectivity had a time lag of 5 ms, and panels B and D show results when the connectivity had a time lag of 25 ms. All results are shown for average reference (left) and Laplacian (right). Topographical maps show connectivity strength of all electrodes with electrode Fz (the “seed” electrode). Time–frequency plots show connectivity between electrodes Fz and Pz (see black/white circled electrodes). Overlaid on all plots is alpha-band (average from 8.9 Hz to 11.4 Hz) connectivity. The dotted white line corresponds to a connectivity strength of 0 and the top of the plot corresponds to connectivity of 1 (see right-side Y-axis label). All topographical and time–frequency plots are on the same color scale (see center bar). Any connectivity results anterior to the “ear-to-ear line” can be considered volume conduction artifacts.

will transiently drop to near-zero, regardless of how clustered the distribution is.

This theoretical and simulated point leads one to wonder whether such frequency non-stationarities exist in real data, and whether phase connectivity is meaningful given such non-stationarities. In fact, time-varying fluctuations in peak frequency (so-called “frequency sliding”; Cohen, 2014a) have been demonstrated in empirical data at the level of scalp M/EEG and intracranial recordings (Ahissar et al., 2001; Foffani et al., 2005; Rudrauf et al., 2006; Roberts et al., 2013), are expected to arise from the fundamental neurophysiological relationship between synaptic input strength and neuronal firing rates (Cohen, 2014a), and may be used to modulate long-range connectivity (Hoppensteadt and Izhikevich, 1998). How these non-stationarities relate to phase connectivity is a more complex issue. Nonetheless, simulation studies show that inter-neuronal communication is robust to modest frequency mismatches (Sancristóbal et al., 2014).

4.4. Functional connectivity in exploratory vs. hypotheses-driven analyses

Before offering recommendations for when ISPC vs. dPLI is most appropriate, it is useful to discuss ways of using connectivity analyses, and the implications for Type-I vs. Type-II errors. Broadly speaking, functional connectivity can be examined in hypothesis-driven analyses and in exploratory data-driven analyses. Usually (though not always), hypothesis-driven analyses involve a relatively small number of statistical tests amongst a small number of

electrodes and time–frequency regions that are selected based on a priori theoretical motivation. Exploratory analyses, on the other hand, usually involve a large number of statistical tests over many (possibly thousands of) electrode pairs, frequency bands, and time windows.

Determining whether an analysis is hypothesis-driven vs. exploratory is important for determining the appropriate statistical threshold and the appropriate connectivity method. In hypothesis-driven analyses, maximal statistical sensitivity to detect theoretically motivated findings should be desired, even if it comes with the risk of increased chances for Type-I errors (false positives, or having a true null result being incorrectly labeled as a significant effect). In contrast, in exploratory analyses, precise interpretations of individual findings might be difficult due to a lack of theoretical framework, or an imprecise theory. For such analyses, Type-I errors should be avoided whenever possible, even if it comes at the expense of increased risk of Type-II errors (failing to identify a true but perhaps subtle effect).

In practice, it is difficult to minimize both Type-I and Type-II errors, and thus one must be willing to tolerate an increased risk in one in order to decrease the other. ISPC increases the risk of Type-I errors while decreasing the risk of Type-II errors because it is robust to time lag, frequency mismatches, and frequency non-stationarities, but can mislabel volume conducted effects as “connectivity.” In contrast, wPLI (and other phase-lag-based connectivity methods) increase the risk of Type-II errors while decreasing the risk of Type-I errors, because they will not incorrectly identify volume conducted artifacts as connectivity,

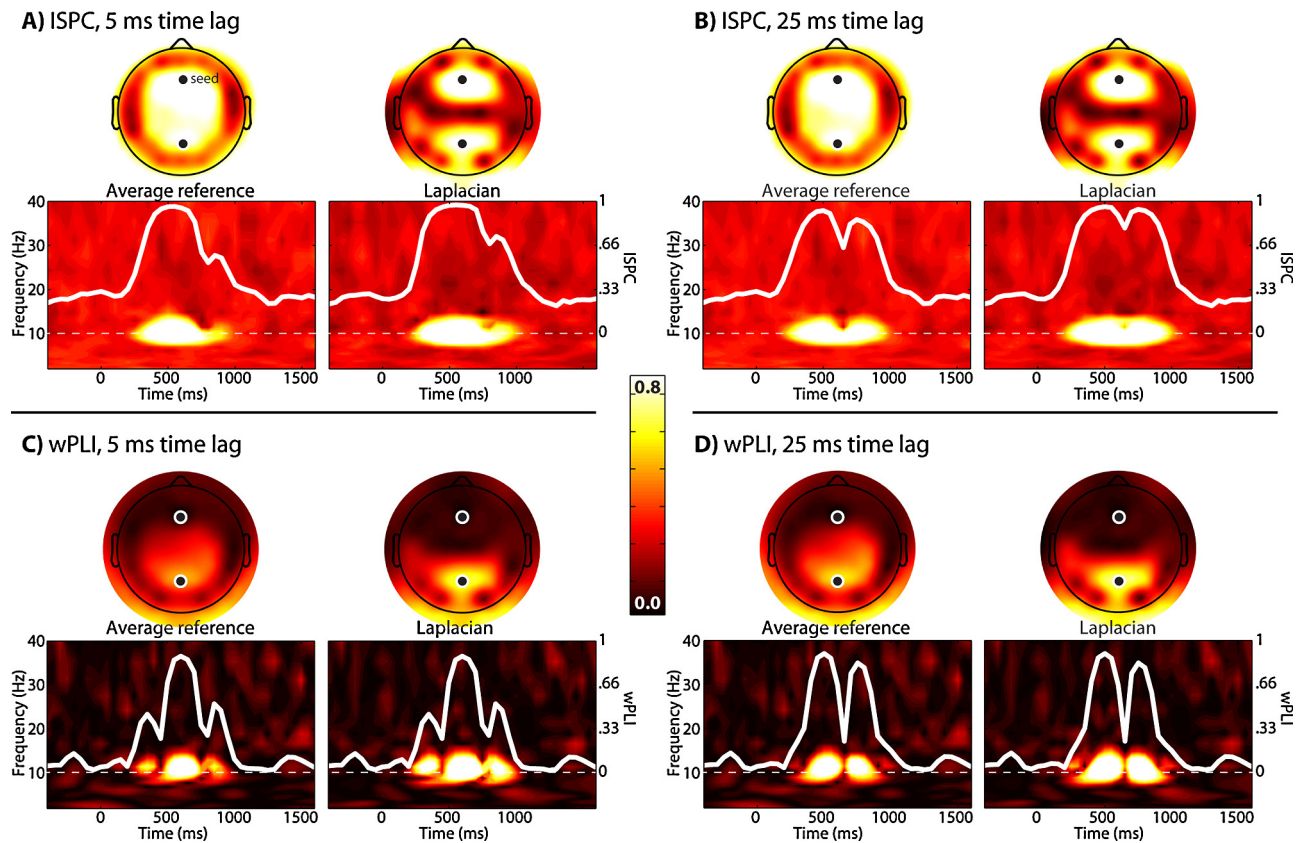


Fig. 5. Results of simulation 2, in which both dipoles oscillated at a constant but different (10 or 12 Hz) frequency. See Fig. 4 for explanation.

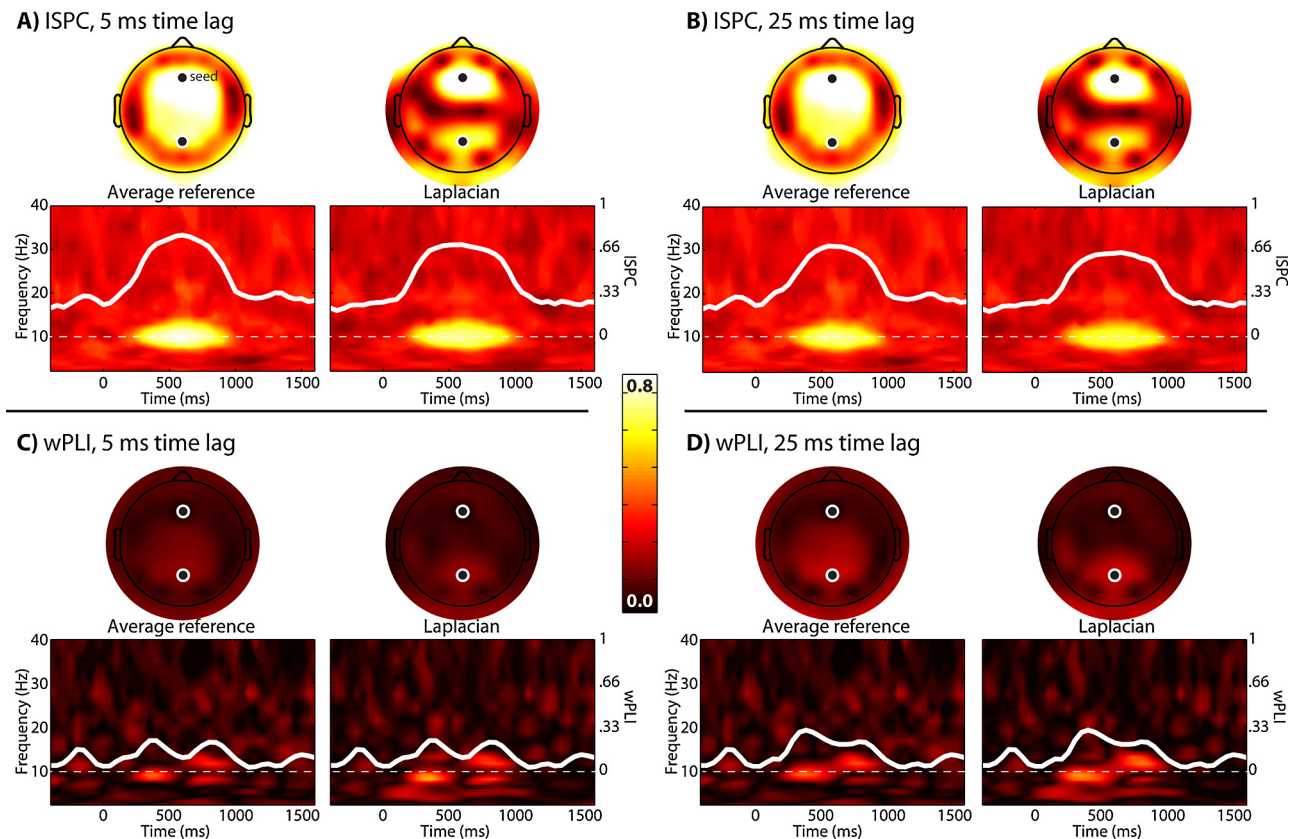


Fig. 6. Results of simulation 3a, in which both dipoles oscillated at time-varying frequencies with a mean 10 Hz and a dispersion of 2 Hz. See Fig. 4 for explanation.

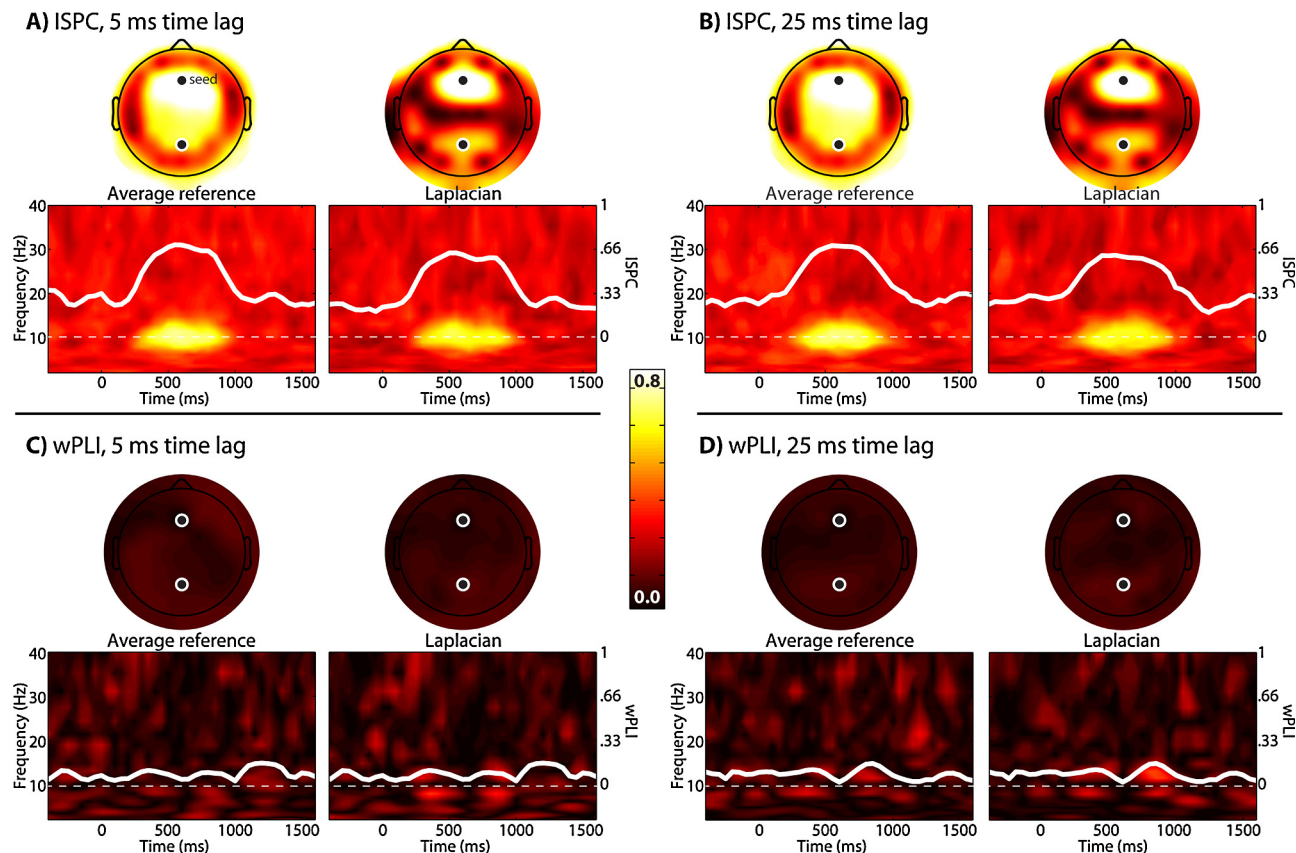


Fig. 7. Results of simulation 3b, in which both dipoles oscillated at time-varying frequencies with a mean 10 Hz and a dispersion of 4 Hz. See Fig. 4 for explanation.

but will under-estimate or fail to identify true connectivity when there are small time lags (particularly in combination with noise), frequency mismatches, or frequency non-stationarities. This limitation is not frequently discussed in the literature, but may be part of the motivation behind the continual development of phase-lag-based measures (including PLI, wPLI, dwPLI, imaginary coherence, corrected imaginary coherence, and phase-slope-index), whereas there is only one dominant phase-clustering-based measure (ISPC, though it is also referred to as phase-locking value/factor/coherence/correlation).

4.5. Recommendations for phase-based connectivity analyses in EEG data

Based on the results presented here, the following procedure is recommended for EEG phase-based connectivity analyses. For strict hypothesis-testing, use ISPC (when appropriate, in combination with follow-up tests to determine whether the effect may reflect volume conduction, as explained below). For exploratory data-driven studies, particularly those involving all-to-all (or some-to-all) analyses, start with the wPLI (or other phase-lag-based measure) to identify electrodes/frequencies that might show significant connectivity. Thereafter, if the research question concerns the timing of connectivity or condition differences in connectivity, ISPC should be used to avoid biases in wPLI.

When using wPLI, it is recommended to average wPLI results over a fairly broad time–frequency range, rather than interpreting wPLI results in a narrow frequency band or restricted time window. The averaging will help reduce wPLI fluctuations, which can be volatile in some situations (see, e.g., Fig. 9).

Concerning spatial filtering, the Laplacian is strongly recommended for electrode-level connectivity analyses. One might even

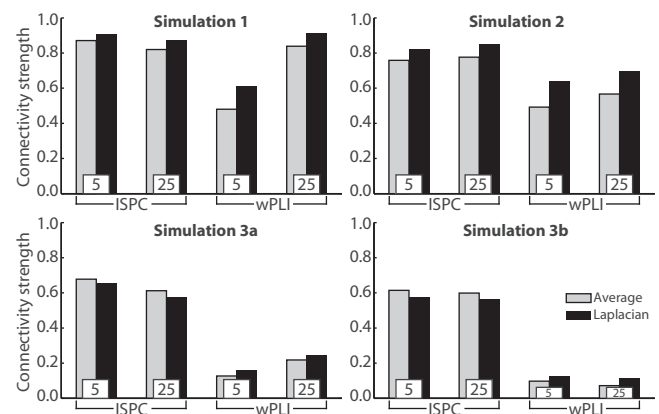


Fig. 8. Bar plots summarize connectivity strength results from Figs. 4 to 7; the results are replotted here for quick and convenient comparison. Each bar depicts the average ISPC or wPLI between electrodes Fz and Pz in a time–frequency window of 8.9–11.4 Hz and 200–800 ms. The number inset (5 or 25) refers to the time lag in ms.

say is it a prerequisite for interpreting ISPC results. Source-level spatial filters such as beamforming may improve the interpretation of the localization of brain regional interactions, but beamforming alone does not eliminate volume conduction artifacts (Sekihara et al., 2011). One of the main advantages of the Laplacian over source space analyses is that it requires few parameters and is based on few assumptions (Srinivasan, 1999; Nunez and Srinivasan, 2005). The Laplacian is likely to be useful for wPLI analyses due to increased topographical localization, but is not necessary for interpreting the results.

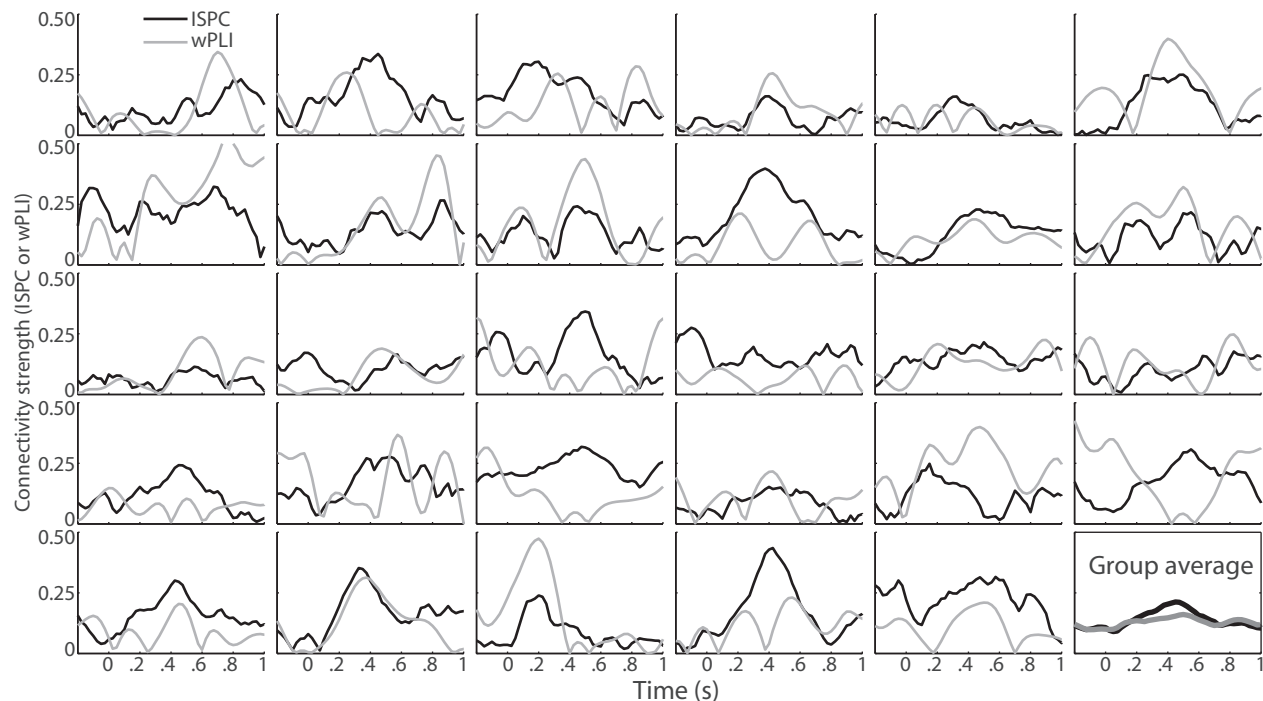


Fig. 9. Comparison of ISPC and wPLI in real human scalp EEG data. Each panel shows results from a single subject; the bottom-right-most panel shows the average across all subjects. The lines correspond to connectivity measured at 6 Hz between electrodes FCz and Pz during trials in which subjects made an erroneous response. The Y-axis scaling is the same for all plots. Time = 0 is stimulus onset.

4.6. Dissociating volume conduction from true connectivity without PLI

Although with ISPC, it may be difficult to know with complete certainty that a connectivity finding is not influenced by volume conduction, there are several analyses that can be used to determine whether a connectivity result is likely to reflect a true brain regional interaction, or whether it can be attributed to volume conduction.

Two preventative measures are recommended. First, EEG data should be spatially filtered using the Laplacian (this transformation should be done in the time domain, prior to time–frequency decomposition). Second, the connectivity time series can be computed as percent change from a baseline to remove residual tonic volume conduction artifacts that are not modulated by the task (see ISPC time courses in Figs. 4–7).

After results have been obtained, several additional follow-up tests can be applied. First, the time course of connectivity can be compared with the time course of power; volume conduction predicts that connectivity and power are nearly perfectly correlated. Second, peak frequencies can be compared between the two electrodes; volume conduction predicts perfectly matched frequencies. Third, the time lag of the connectivity can be computed; volume conduction predicts either 0 or π time lag (depending on the positions of the electrodes with respect to the dipole). Failing to confirm predictions of volume conduction increase the confidence in the ISPC connectivity result without concern for Type-II errors.

Acknowledgments

Thanks to Daan van Es for assistance with data collection. This work was funded by a VIDI grant from the NWO (452-09-003) (Dutch Science Funding Agency).

References

- Ahissar E, Nagarajan S, Ahissar M, Protopapas A, Mahncke H, Merzenich MM. Speech comprehension is correlated with temporal response patterns recorded from auditory cortex. *Proc Natl Acad Sci U S A* 2001;98:13367–72.
- Appelbaum LG, Smith DV, Boehler CN, Chen WD, Woldorff MG. Rapid modulation of sensory processing induced by stimulus conflict. *J Cogn Neurosci* 2011;23:2620–8.
- Bush P, Sejnowski T. Inhibition synchronizes sparsely connected cortical neurons within and between columns in realistic network models. *J Comput Neurosci* 1996;3:91–110.
- Cabral J, Kringelbach ML, Deco G. Exploring the network dynamics underlying brain activity during rest. *Prog Neurobiol* 2014;114:102–31.
- Cohen MX. Fluctuations in oscillation frequency control spike timing and coordinate neural networks. *J Neurosci* 2014a;34(27):8988–98.
- Cohen MX. *Analyzing neural time series data: theory and practice*. Cambridge: MIT Press; 2014b.
- Cohen MX. Comparison of different spatial filters applied to EEG data: a case study of error processing. *Int J Psychophysiol* 2014c, in press.
- Delorme A, Makeig S. EEGLAB: an open source toolbox for analysis of single-trial EEG dynamics including independent component analysis. *J Neurosci Methods* 2004;134:9–21.
- Foffani G, Bianchi AM, Baselli G, Priori A. Movement-related frequency modulation of beta oscillatory activity in the human subthalamic nucleus; 2005.
- Fries P. A mechanism for cognitive dynamics: neuronal communication through neuronal coherence. *Trends Cogn Sci* 2005;9:474–80.
- Gramfort A, Papadopoulos T, Olivi E, Clerc M. OpenMEEG: opensource software for quasistatic bioelectromagnetics. *Biomed Eng Online* 2010;9:45.
- Haegens S, Cousijn H, Wallis G, Harrison PJ, Nobre AC. Inter- and intra-individual variability in alpha peak frequency. *Neuroimage* 2014;1–10.
- Hoppensteadt FC, Izhikevich EM. Thalamo-cortical interactions modeled by weakly connected oscillators: could the brain use FM radio principles? In: *BioSystems*; 1998. p. 85–94.
- Hutchinson RM, Womelsdorf T, Allen EA, Bandettini PA, Calhoun VD, Corbetta M, et al. Dynamic functional connectivity: promise, issues, and interpretations. *Neuroimage* 2013;80:360–78.
- Kaplan AY, Fingelkurts AA, Fingelkurts SV, Darkhovsky BS. Nonstationary nature of the brain activity as revealed by EEG/MEG: methodological, practical and conceptual challenges. *Signal Process* 2005;85:2190–212.
- Nolte G, Bai O, Wheaton L, Mari Z, Vorbach S, Hallett M. Identifying true brain interaction from EEG data using the imaginary part of coherency. *Clin Neurophysiol* 2004;115:2292–307.
- Nunez PL, Srinivasan R. *Electric fields of the brain: the neurophysics of EEG*. 2nd ed. USA: Oxford University Press; 2005.

- Ray S, Maunsell JHR. Differences in gamma frequencies across visual cortex restrict their possible use in computation. *Neuron* 2010;67:885–96.
- Roberts MJ, Lowet E, Brunet NM, Ter Wal M, Tiesinga P, Fries P, et al. Robust gamma coherence between macaque V1 and V2 by dynamic frequency matching. *Neuron* 2013;78:523–36.
- Rudrauf D, Douiri A, Kovach C, Lachaux J-P, Cosmelli D, Chavez M, et al. Frequency flows and the time–frequency dynamics of multivariate phase synchronization in brain signals. *Neuroimage* 2006;31:209–27.
- Sancristóbal B, Vicente R, Garcia-Ojalvo J. Role of frequency mismatch in neuronal communication through coherence. *J Comput Neurosci* 2014;37(2):193–208.
- Sekihara K, Nagarajan SS, Poeppel D, Marantz A. Performance of an MEG adaptive-beamformer technique in the presence of correlated neural activities: effects on signal intensity and time-course estimates. *IEEE Trans Biomed Eng* 2002;49:1534–46.
- Sekihara K, Owen JP, Trisno S, Nagarajan SS. Removal of spurious coherence in MEG source-space coherence analysis. *IEEE Trans Biomed Eng* 2011;58:3121–9.
- Sporns O. *Networks of the brain*. Cambridge: MIT Press; 2010.
- Srinivasan R. Methods to improve the spatial resolution of EEG. *Int J Bioelectromagn* 1999;1:102–11.
- Srinivasan R, Winter WR, Ding J, Nunez PL. EEG and MEG coherence: measures of functional connectivity at distinct spatial scales of neocortical dynamics. *J Neurosci Methods* 2007;166:41–52.
- Srinivasan R, Winter WR, Nunez PL. Source analysis of EEG oscillations using high-resolution EEG and MEG. *Prog Brain Res* 2006;159:29–42.
- Stam CJ, Nolte G, Daffertshofer A. Phase lag index: assessment of functional connectivity from multi channel EEG and MEG with diminished bias from common sources. *Hum Brain Mapp* 2007;28:1178–93.
- Tadel F, Baillet S, Mosher JC, Pantazis D, Leahy RM. Brainstorm: a user-friendly application for MEG/EEG analysis. *Comput Intell Neurosci* 2011, <http://www.hindawi.com/journals/cin/2011/879716/cta/>.
- Tognoli E, Kelso JAS. Spectral dissociation of lateralized pairs of brain rhythms; 2013. p. 6.
- Varela F, Lachaux JP, Rodriguez E, Martinerie J. The brainweb: phase synchronization and large-scale integration. *Nat Rev Neurosci* 2001;2:229–39.
- Vinck M, Oostenveld R, van Wingerden M, Battaglia F, Pennartz CMA. An improved index of phase-synchronization for electrophysiological data in the presence of volume-conduction, noise and sample-size bias. *Neuroimage* 2011;55:1548–65.
- Winter WR, Nunez PL, Ding J, Srinivasan R. Comparison of the effect of volume conduction on EEG coherence with the effect of field spread on MEG coherence. *Stat Med* 2007;26:3946–57.